·Basic Research·

Cytotoxicity of pilocarpine to human corneal stromal cells and its underlying cytotoxic mechanisms

Xiao-Long Yuan, Qian Wen, Meng-Yu Zhang, Ting-Jun Fan

Laboratory for Corneal Tissue Engineering, College of Marine Life Sciences, Ocean University of China, Qingdao 266003, Shandong Province, China

Correspondence to: Ting-Jun Fan. Laboratory for Corneal Tissue Engineering, College of Marine Life Sciences, Ocean University of China, Qingdao 266003, Shandong Province, China. tjfan@ouc.edu.cn

Received: 2015-03-18 Accepted: 2015-09-29

Abstract

• AIM: To examine the cytotoxic effect of pilocarpine, an anti-glaucoma drug, on human corneal stromal (HCS) cells and its underlying cytotoxic mechanisms using an *in vitro* model of non-transfected HCS cells.

• METHODS: After HCS cells were treated with pilocarpine at a concentration from 0.15625 g/L to 20.0 g/L, their morphology and viability were detected by light microscopy and MTT assay. The membrane permeability, DNA fragmentation and ultrastructure were examined by acridine orange (AO)/ethidium bromide (EB) double-staining. DNA electrophoresis and transmission electron microscopy (TEM), cell cycle, phosphatidylserine (PS) orientation and mitochondrial transmembrane potential (MTP) were assayed by flow cytometry (FCM). And the activation of caspases was checked by ELISA.

• RESULTS: Morphology observations and viability assay showed that pilocarpine at concentrations above 0.625 g/L induced dose- and time-dependent morphological abnormality and viability decline of HCS cells. AO/EB double-staining, DNA electrophoresis and TEM noted that pilocarpine at concentrations above 0.625 g/L induced dose- and/or time-dependent membrane permeability elevation, DNA fragmentation, and apoptotic body formation of the cells. Moreover, FCM and ELISA assays revealed that 2.5 g/L pilocarpine also induced S phase arrest, PS externalization, MTP disruption, and caspase-8, -9 and -3 activation of the cells.

• CONCLUSION: Pilocarpine at concentrations above 0.625 g/L (1/32 of its clinical therapeutic dosage) has a dose- and time-dependent cytotoxicity to HCS cells by inducing apoptosis in these cells, which is most probably regulated by a death receptor-mediated mitochondrion-dependent signaling pathway.

• KEYWORDS: pilocarpine; cytotoxicity; human corneal stromal cells; apoptosis; mitochondrion

DOI:10.18240/ijo.2016.04.05

Yuan XL, Wen Q, Zhang MY, Fan TJ. Cytotoxicity of pilocarpine to human corneal stromal cells and its underlying cytotoxic mechanisms. *Int J Ophthalmol* 2016;9(4):505-511

INTRODUCTION

Human corneal stroma (HCS) is composed of highly organized extracellular matrix (ECM) and mitotically quiescent HCS cells [1]. The specialized HCS cells play important roles in maintaining corneal transparency and wound healing by synthesizing ECM components [2-4]. Damages to corneal epithelium and/or stroma from trauma and drugs often induce apoptosis of HCS cells [5], and excessive loss of HCS cells usually results in serious complications[6]. Therefore, it will be of great significance to characterize the cytotoxicity of topical drugs to the cornea and the underlying cytotoxic mechanisms, especially to HCS. Pilocarpine, a cholinergic anti-glaucoma drug, is widely and chronically used in eye clinic for glaucoma treatment [7-9]. Unfortunately, it has been reported that repeated and prolonged medication of pilocarpine often results in adverse effects, such as seizures, posterior synechiae, iris cysts, and so on [10-13]. However, the cytotoxicity of pilocarpine to HCS remains unkown due to the lack of an *in vitro* model of HCS cells that can be used for cytotoxicity investigations [14]. Recently, a non-transfected HCS cell line was successfully established in our laboratory [15], and it makes it possible to study intensively the cytotoxicity of pilocarpine to HCS cells and the underlying mechanisms *in vitro*. The present study was intended to investigate the cytotoxicity of Pilocarpine to HCS and the underlying cellular and molecular mechanisms using an *in vitro* model of HCS cells.

MATERIALS AND METHODS

Materials Pilocarpine ($C_{11}H_{16}N_2O_2$) was purchased from Alfa Aesar (Tianjin, China). HCS cells, from the nontransfected HCS cell line (utHCSC01) established previously in our laboratory [15], were maintained and cultured in 10% bovine calf serum (BCS, Invitrogen, Carlsbad, CA, USA)-containing Dulbecco's modified Eagle medium: Ham's nutrient mixture F-12 medium (DMEM/F12, 1:1) (Invitrogen, Carlsbad, CA, USA) at 37℃ in 25 cm^2 culture flasks (Nunc, Copenhagen, Denmark) as described previously.

Experimental Design After cultured logarithmic HCS cells were treated with pilocarpine at concentrations from 0.3125 g/L to 20.0 g/L, and the morphology, viability, and cell cycle were checked by light microscopy, MTT assay, and flow cytometry (FCM) using propidium iodide (PI) staining for cytotoxicity evaluation. The membrane permeability, phosphatidylserine (PS) orientation, DNA integrality, and ultrastructure were examined by acridine orange (AO)/ethidium bromide (EB) double-staining, FCM using Annexin-V/PI staining, DNA electrophoresis, and transmission electron microscopy (TEM) for apoptosis characterization. And the caspase activation and mitochondrial transmembrane potential (MTP) was assayed by ELISA and FCM using JC-1 staining for apoptosis signaling pathway investigation. HCS cells cultured in the same medium without any Pilocarpine addition at the same time point were used as controls in all experiments.

Methods

Morphological observation Cell morphology was observed by light microscopy. HCS cells were harvested from culture flasks by trypsin digestion and centrifugation as described previously [15], and inoculated into a 24-well culture plate (Nunc) at 6.0×10^4 cells/well and grown at 37℃ in a 5% CO_2 incubator. When the cells reached to logarithmic phase, their culture medium was replaced entirely with 0.3125-20.0 g/L pilocarpine-containing 10% BCS-DMEM/F12 medium. The morphology and growth status of the cells were monitored successively with a TS-100 light microscope (Nikon, Tokyo, Japan) at a 4h interval.

Cell viability assay Cell viability was determined by 3-(4,5-dimethyl-2-thiazolyl)-2,5-diphenyl-2-H-tetrazolium bromide (MTT) assay as described previously [16]. Briefly, HCS cells were inoculated into a 96-well culture plate (Nunc) at a density of 1×10^4 cells/100 μL/well, and were cultured and treated as described above. At a 4h interval, the pilocarpine-containing medium was replaced entirely with 100 μL serum-free DMEM/F12 medium containing 1.0 g/L MTT (Sigma-Aldrich, St. Louis, MO, USA), and the cells were incubated at 37℃ in the dark for 4h. After the MTT-containing medium was discarded with caution, 150 μL dimethyl sulfoxide (DMSO; Sigma-Aldrich) was added to dissolve the produced formazan crystals at 37℃ in the dark for 15min, and the absorbance at 490 nm was measured with a Multiskan GO microplate reader (Thermo Scientific, MA, USA).

Plasma membrane permeability detection Plasma membrane permeability of HCS cells was measured by AO/EB double-staining as described previously [16]. In brief, HCS cells in a 24-well culture plate (Nunc) were cultured, treated and harvested as described above. After stained with 100 μg/mL AO/EB (Sigma-Aldrich) (1:1) solution for 1min, the cell suspension was observed under a Ti-S fluorescent microscope (Nikon, Tokyo, Japan). HCS cells with red or orange nuclei were designated as apoptotic cells while those with green nuclei as non-apoptotic cells, and at least 300 cells from several random fields were counted in each group. The apoptotic ratio was calculated according to the formula of "Apoptotic rate (%)=Apoptotic cells/(Apoptotic cells+non-apoptotic cells)×100%".

DNA electrophoresis DNA fragmentation was detected by agarose gel electrophoresis according to the method reported previously [17]. Briefly, HCS cells in 25 cm^2 flasks (Nunc) were cultured, treated and harvested as described above. The DNA from 1.4×10^5 cells was isolated with a Quick Tissue/Culture Cells Genomic DNA Extraction Kit (Dongsheng Biotech, Guangzhou, Guangdong Province, China). The DNA extracts from each group was electrophoresed on 1% agarose gel (15 V, 4h), stained with 0.5 mg/L ethidium bromide for 10min, and observed with an EC3 imaging system (UVP, LLC Upland, CA, USA).

Ultrastructural observation Ultrastructure of HCS cells was checked by transmission electron microscopy (TEM) as described previously [17]. In brief, HCS cells in 25 cm^2 flasks were cultured, treated with 2.5 g/L pilocarpine and harvested as described above. After fixed successively with 4% glutaraldehyde and 10 g/L osmium tetroxide, the cells were dehydrated and embedded in epoxy resin. Ultrathin sections were stained with 20 g/L uranyl acetate-lead citrate and observed with an H700 TEM (Hitachi, Tokyo, Japan).

Flow cytometry analyses The cell cycle status, PS orientation and MTP were detected and analyzed by FCM as reported previously [16]. Briefly, HCS cells in 6-well plates (Nunc) were cultured, treated with 2.5 g/L pilocarpine and harvested as described above. After washed twice with 1 mL phosphate-buffered saline (PBS), the cells were fixed with 70% alcohol at 4℃ overnight. Then the cells were stained with PI (BD Biosciences, San Jose, CA, USA) for cell cycle assay, stained with Annexin-V/PI using FITC Annexin V Apoptosis Detection Kit I (BD Biosciences) for PS externalization assay, and stained with 10 μg/mL 5,5',6,6'-tetrachloro-1,1',3,3'-tetraethybenzimida (JC-1; Sigma-Aldrich) for MTP assay, respectively. The stained cells, 3.6×10^5 cells at a minimum, were detected by a FACScan flow cytometer and analyzed with CXP analysis software (BD Biosciences).

Caspase activation assay Caspase activation was measured by enzyme-linked immunosorbent assay (ELISA) as described previously [16]. Briefly, HCS cells in 6-well plates (Nunc) were cultured, treated with 2.5 g/L pilocarpine and harvested as described above. Whole-cell protein extracts from 5.0×10^5 cells were prepared by utilizing a RIPA lysis kit (Biotime, Beijing, China) according to the manufacturer's instructions. About 100 μL supernatant was coated into high-binding 96-well microtiter plates (Nunc) overnight at 4℃. After blocked with 5% non-fat milk (BD Biosciences), the wells were incubated with rabbit anti-human caspase-3,

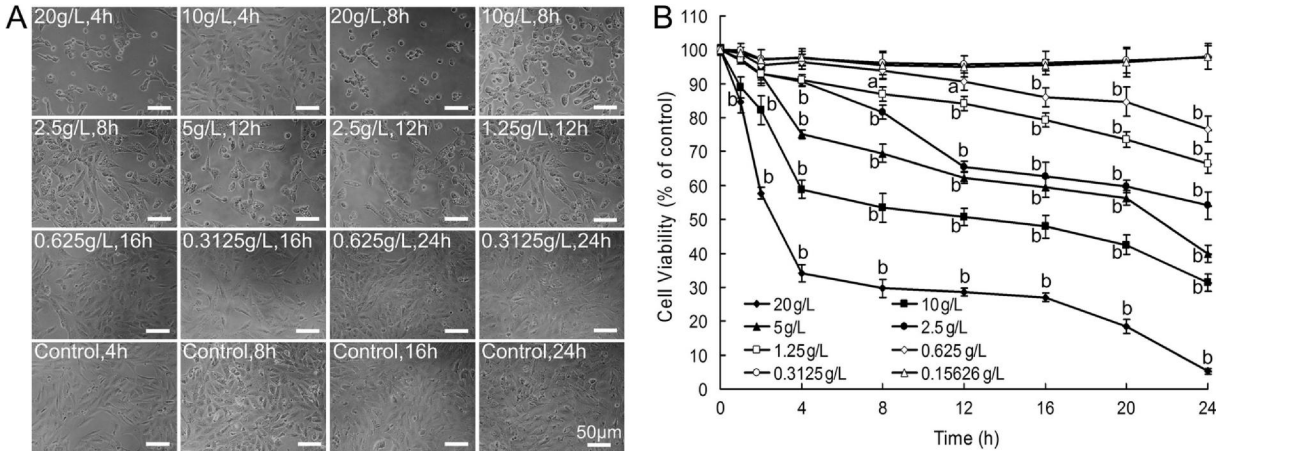

Figure 1 Dose and time dependent cytotoxicity of pilocarpine to HCS cells Cultured HCS cells were treated with the indicated concentration and exposure time of pilocarpine. A: Light microscopy. One representative photograph from three independent experiments was shown. Scale bar=50 μm. B: MTT assay. The cell viability of pilocarpine-treated HCS cells in each group was expressed as percentage (mean±SD) of 490 nm absorbance compared to its corresponding control (n =3). ^{a}P <0.05, ^{b}P <0.01 versus control.

-8, and -9 (active form) antibodies (1:500) (Biosynthesis Biotechnology, Beijing, China), and the HRP-conjugated goat anti-rabbit secondary antibody (1:3000) (cwBiotech, Nanjing, China), respectively, at 37℃ for 2h. A colorimetric reaction was induced by 1% tetramethylbenzidine (TMB) for 25min in the dark at room temperature. Color development was stopped with 50 μL H_2SO_4 (0.5 mol/L), and the 490 nm absorbance of each well was measured using a Multiskan GO microplate reader (Thermo Scientific).

Statistical Analysis Each experiment was repeated 3 times independently. Data are shown as mean±standard deviation (SD). Group comparisons were conducted using one-way analysis of variance (ANOVA) using SPSS 21.0 software (Chicago, IL, USA). Differences to controls were considered statistically significant when P <0.05.

RESULTS

Cytotoxic Effect of Pilocarpine on Human Corneal Stromal Cells To evaluate the cytotoxicity of pilocarpine, the morphology and viability of HCS cells were examined by light microscopy and MTT assay, respectively. Morphological observations showed that HCS cells exposed to pilocarpine at a concentration from 0.625 to 20 g/L exhibited dose- and time-dependent proliferation retardation and morphological abnormality such as cellular shrinkage, cytoplasmic vacuolation, detachment from culture matrix, and eventually death , while no obvious difference was observed between those exposed to pilocarpine below the concentration of 0.625 g/L and controls (Figure 1A). Results of MTT assay revealed that the cell viability of HCS cells decreased with time and concentration after exposing to pilocarpine above the concentration of 0.625 g/L (P <0.01 or 0.05), while that of HCS cells treated with pilocarpine below the concentration of 0.625 g/L showed no significant difference to controls (Figure 1B).

Cell Cycle Arrest of Human Corneal Stromal Cells To verify the proliferation retarding mechanisms of pilocarpine, the cell cycle status of HCS cells were examined by FCM using PI staining. Results showed that the number of 2.5 g/L pilocarpine-treated HCS cells in S phase increased from 21.6% of control to 25.7% (P <0.05) at 4h, 30.7% (P <0.01) at 8h, and 56.6% (P <0.01) at 12h, respectively, while that in G1 phase and G2/M phase decreased with time (P <0.01 or 0.05), respectively, when compared with controls (Figure 2).

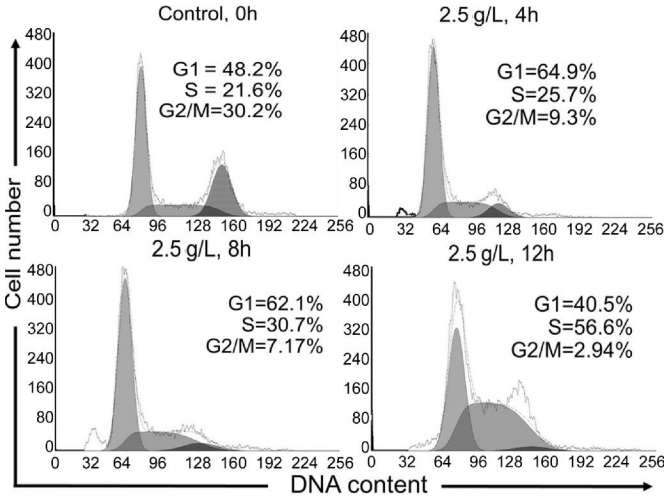

Figure 2 Pilocarpine induced cell cycle arrest of HCS cells Cultured HCS cells were treated with the indicated concentration and exposure time of pilocarpine, and their cell cycle status was checked by FCM with PI staining. One representative photograph from three independent experiments was shown.

Plasma Membrane Abnormality of Human Corneal Stromal Cells To examine whether the cytotoxicity of pilocarpine was achieved by inducing apoptosis, plasma membrane permeability and PS orientation of pilocarpine-treated HCS cells were detected by AO/EB double-staining and FCM using Annexin V/PI staining, respectively. Our results of AO/EB double-staining displayed that pilocarpine at concentrations above 0.625 g/L could elevate the plasma

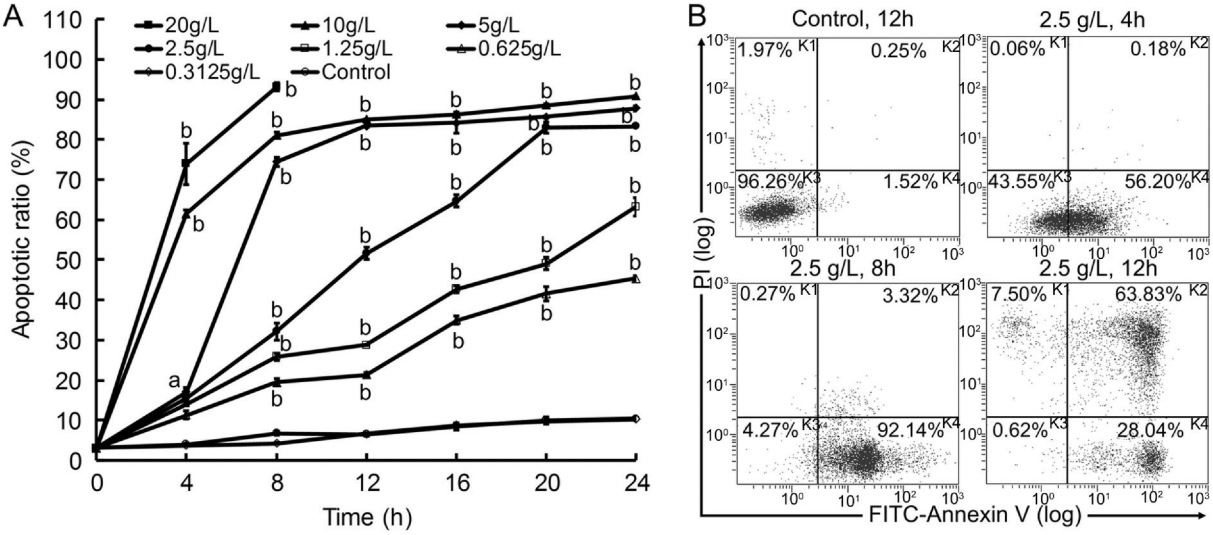

Figure 3 Pilocarpine induced plasma membrane abnormality of HCS cells Cultured HCS cells treated with the indicated concentration and exposure time of pilocarpine. A: AO/EB double staining. The apoptotic ratio was calculated as percentage (mean±SD) of the total number of cells based on the permeability elevation of plasma membrane of HCS cells (n=3). Data are presented as mean±SD. [a] P<0.05, [b] P< 0.01 versus control. B: FCM using Annexin V/PI staining. The cell number of HCS cells in each group was expressed as percentage of the total number of cells. One representative photograph from three independent experiments was shown. K1: Necrosis; K2: Late apoptosis; K3: Normal cell; K4: Early apoptosis. The cells in K2 and K4 phase exhibit PS externalization.

membrane permeability of HCS cells in a dose- and time-dependent manner (P <0.01 or 0.05), while that of HCS cells treated with pilocarpine below 0.625 g/L showed no significant difference to controls (Figure 3A). Results of FCM using Annexin V/PI staining showed that HCS cells treated with 2.5 g/L pilocarpine exhibited time-dependent increase of PS externalization when compared with its corresponding control (Figure 3B). The number of early and late apoptotic cells (PS externalized cells) increased from 1.77% of control to 56.38% (P <0.01) at 4h, 95.46% (P< 0.01) at 8h, and 91.87% (P <0.01) at 12h, respectively.

DNA Fragmentation and Ultrastructural Abnormality of Human Corneal Stromal Cells To verify the apoptosis inducing effect of pilocarpine, DNA fragmentation and ultrastructure of pilocarpine-treated HCS cells was characterized by DNA electrophoresis and TEM, respectively. Results of DNA electrophoresis indicated that the genomic DNA extracted from pilocarpine-treated HCS cells was fragmented into a highly dispersed state, and typical DNA ladders were found in 0.625-2.5 g/L pilocarpine-treated cells, while no DNA ladder was found in those of controls (Figure 4A). Moreover, TEM observations postulated that 2.5 g/L pilocarpine-treated HCS cells exhibited ultrastructural disorganizations, including cytoplasmic vacuolation, mitochondrion swelling, chromatin condensation, and apoptotic body formation (Figure 4B).

Caspase Activation and Mitochondrial Transmembrane Potential Disruption of Human Corneal Stromal Cells To postulate the possible triggering pathways involved in pilocarpine-induced apoptosis, caspase activation and MTP disruption was further measured by ELISA using antibodies to the active form of caspase-3, -8 and -9 and FCM using JC-1 staining, respectively. Results of ELISA revealed that 2.5 g/L pilocarpine could activate caspase-8, -9, and -3 in HCS cells successively(P<0.01 or 0.05), of which caspase-8 was first activated to its peak value at 2h(P<0.01), caspase-9 activated to its peak value at 4h (P <0.01), while caspase-3 was activated continually during the monitoring period (P < 0.01 or 0.05) (Figure 5A). Moreover, FCM using JC-1 staining indicated that 2.5 g/L pilocarpine could induce MTP disruption in HCS cells, and the number of JC-1 positive cells (MTP-disrupted cells) increased from 0.97% of control to 26.30% (P <0.01) at 4h, 51.42% (P <0.01) at 8h, and 82.55% (P <0.01) at 12h, respectively (Figure 5B).

DISCUSSION

Anti-glaucoma drugs, such as latanoprost, have been reported to have toxic effects on HCS and result in reduction in central corneal thickness and even keratoconus progression[18-19]. However, the effect of pilocarpine, a widely used anti-glaucoma drug in eye clinic, on HCS remains unclear. To provide cytotoxic references for prospective therapeutic interventions of anti-glaucoma drugs, the present study was intended to investigate the cytotoxicity of pilocarpine to HCS and its possible cellular and molecular mechanisms using an *in vitro* model of non-transfected HCS cells[15].

To evaluate the cytotoxicity of pilocarpine, the morphology, viability and cell cycle status of pilocarpine-treated HCS cells were examined at first in this study. We found that pilocarpine at concentrations above 0.625 g/L (1/32 of its clinical therapeutic dosage) could induce dose- and time-dependent morphological abnormality, proliferation

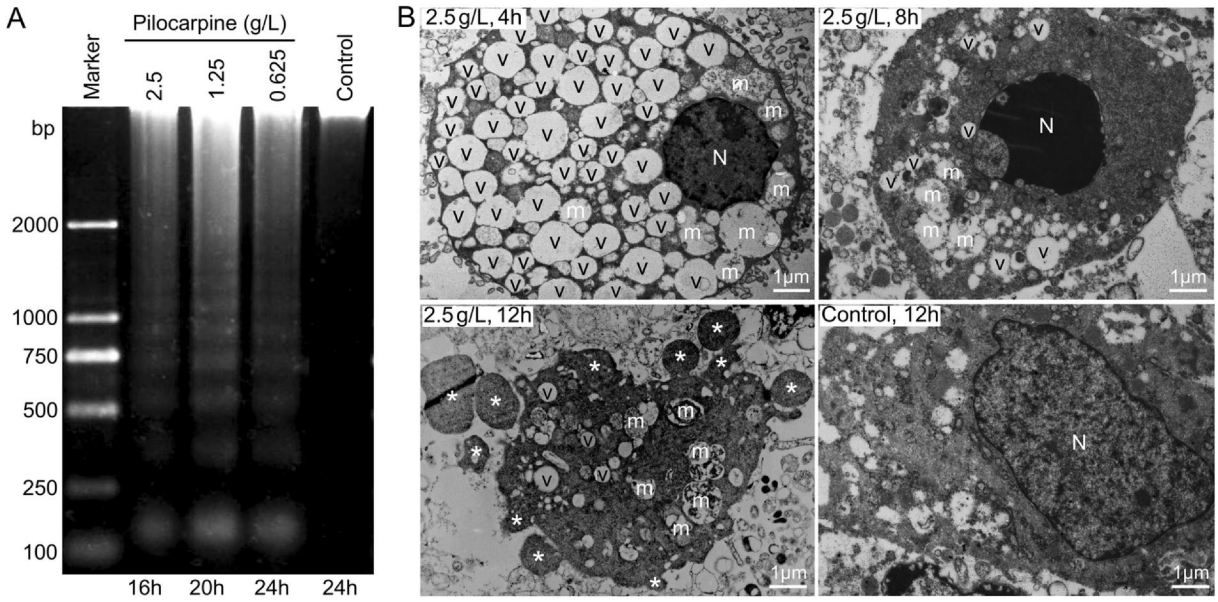

Figure 4 Pilocarpine induced DNA fragmentation and ultrastructural abnormality of HCS cells Cultured HCS cells were treated with the indicated concentration and exposure time of pilocarpine. A: DNA electrophoresis. DNA isolated from HCS cells was electrophoresed in 1% agarose gel, and dispersed DNA ladders were shown. B: TEM images. One representative photograph from three independent experiments was shown. N: Nucleus; v: Vacuoles; m: Swollen mitochondrion; a: Apoptotic body.

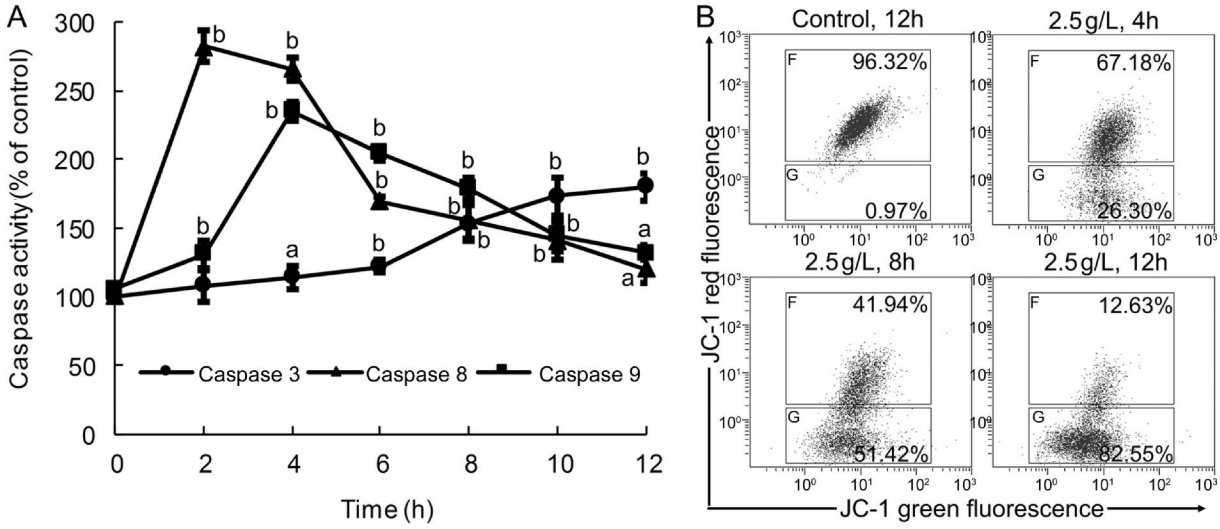

Figure 5 Pilocarpine induced caspase activation and MTP disruption of HCS cells Cultured HCS cells were treated with the indicated exposure time of 2.5 g/L pilocarpine. A: ELISA. Caspase activation induced by pilocarpine was assayed using the active form of caspase-3, -8 and -9 antibodies. The activation ratio of each group was expressed as percentage (mean±SD) compared to its corresponding control based on 490 nm absorbance (n=3). ^aP<0.05, ^bP<0.01 versus control. B: FCM images of JC-1 staining. JC-1 in mitochondria with MTP depolarized maintains monomers in green fluorescence, while that in mitochondria with normal MTP incorporates into aggregates in red fluorescence. One representative photograph from three independent experiments was shown. The cell number of MTP disrupted HCS cells in each group was expressed as percentage of the total number of cells.

retardation, and viability decline of HCS cells. Moreover, 0.625 g/L pilocarpine could also induce S phase arrest of HCS cells. Our findings suggest that pilocarpine above 1/32 of its clinical therapeutic dosage has significant cytotoxicity to HCS cells *in vitro*, and S phase arrest is involved in the retarded proliferation of HCS cells induced by pilocarpine. These findings are supported by previously reported cytotoxicity of ophthalmic drugs and anesthetics to human corneal cells [16,20-24]. Since cell viability decline and cell cycle arrest are often related with apoptosis triggered by chemotherapeutic agents [22-25], it can be deduced that the cytotoxic effect of pilocarpine on HCS cells might also be related with apoptosis.

As well postulated previously, plasma membrane permeability elevation, PS externalization, DNA fragmentation and apoptotic body formation are the hallmark features of apoptosis [26-29]. To verify whether the cytotoxicity of pilocarpine was achieved by inducing cell apoptosis, we then investigated the plasma membrane permeability, PS externalization, DNA fragmentation, and apoptotic body

formation of HCS cells using AO/EB double staining, FCM using Annexin V/PI staining, DNA electrophoresis, and TEM, respectively. Our results showed that pilocarpine above concentrations of 0.625 g/L could induce dose- and time-dependent membrane permeability elevation of HCS cells, and 2.5 g/L pilocarpine could also induce PS externalization, DNA fragmentation and apoptotic body formation. As well defined, the key difference between apoptosis and necrosis is the formation of apoptotic bodies with externalized PS in their plasma membrane, which is a vital feature for clearing away the apoptotic cells by phagocytosis [27,29]. Therefore, our findings confirmed that pilocarpine could induce apoptosis of HCS cells *in vitro*. The pilocarpine-induced HCS cell apoptosis is consistent with our previous reports of topical anesthetic- and ophthalmic drug-induced apoptosis in human corneal cells[16,20-24].

As we know, apoptosis is a normal physiological process regulated orderly by intricate pathways, such as the death receptor-mediated extrinsic pathway and the mitochondrion-dependent intrinsic pathway [30-31], which will result in the activation of initiator caspases (caspase-2, -8, -10, and -9) and subsequent activation of executioner caspases (caspase-3, -6, and -7)[32-33]. Meanwhile, MTP disruption is a prerequisite for triggering release of mitochondrion sequestered apoptotic proteins, such as cytochrome c, an indispensable activator of caspase 9, apoptosis inducing factor, and Smac/Diablo[31,34-36]. To postulate the possible apoptosis-triggering pathways of pilocarpine, the activation pattern of caspase-3, -8, and -9 and MTP disruption was further studied by ELISA using antibodies of their active forms and FCM using JC-1 staining, respectively. We found that 2.5 g/L pilocarpine could activate caspase-8, -9, and -3 successively, and induce MTP disruption in a time-dependent manner in HCS cells. Since caspase-8 is an important mediator of tumor necrosis factor receptor 1 (TNFR1)-mediated extrinsic pathway while caspase-9 is a key mediator of the mitochondrion-dependent intrinsic pathway [33,37], our results of the activation of caspase-8, -9, and -3 in pilocarpine-treated HCS cells, combined with MTP disruption, suggest that the pilocarpine-induced HCS cell apoptosis might be triggered via both a death receptor-mediated pathway and a mitochondrion-dependent pathway. The involvement of both an extrinsic and an intrinsic signaling pathway has also been reported in other chemical induced apoptosis[16,21-22,38-39].

In conclusion, pilocarpine above 1/32 of its clinical therapeutic concentration has a dose- and time-dependent cytotoxicity to HCS cells *in vitro*, and its cytotoxicity is achieved by inducing death receptor-mediated mitochondrion-dependent apoptosis. By now, this is the first attempt of investigating the cytotoxicity of pilocarpine to HCS cells and its toxic mechanisms at cellular and molecular levels *in vitro*. Even these findings do not allow predicting clinical inferences *in vivo* directly without further investigations, they provide new insights into the acute cytotoxicity and apoptosis-inducing effect of pilocarpine on HCS cells.

ACKNOWLEDGEMENTS

Foundation: Supported by National High Technology Research and Development Program ("863" Program) of China (No. 2006AA02A132).

Conflicts of Interest: Yuan XL, None; **Wen Q,** None; **Zhang MY,** None; **Fan TJ,** None.

REFERENCES

1 DelMonte DW, Kim T. Anatomy and physiology of the cornea. *J Cataract Refr Surg* 2011;37(3):588-598.

2 Jester JV, Barry PA, Lind GJ, Petroll WM, Garana R, Cavanagh HD. Corneal keratocytes: in situ and in vitro organization of cytoskeletal contractile proteins. *Invest Ophth Vis Sci* 1994;35(2):730-743.

3 Shtein RM, Kelley KH, Musch DC, Sugar A, Mian SI. In vivo confocal microscopic evaluation of corneal wound healing after femtosecond laser-assisted keratoplasty. *Ophthalmic Surg Lasers Imaging* 2012;43(3):205-213.

4 Chien Y, Liao YW, Liu DM, Lin HL, Chen SJ, Chen HL, Peng CH, Liang CM, Mou CY, Chiou SH. Corneal repair by human corneal keratocyte-reprogrammed iPSCs and amphiphatic carboxymethyl-hexanoyl chitosan hydrogel. *Biomaterials* 2012;33(32):8003-8016.

5 Lee KS, Ko DA, Kim ES, Kim MJ, Tchah H, Kim JY. Bevacizumab and rapamycin can decrease corneal opacity and apoptotic keratocyte number following photorefractive keratectomy. *Invest Ophth Vis Sci* 2012;53(12):7645-7653.

6 Wilson SE, Chaurasia SS, Medeiros FW. Apoptosis in the initiation, modulation and termination of the corneal wound healing response. *Exp Eye Res* 2007;85(3):305-311.

7 Yung RL, Francis S. Sjögren's Syndrome in the elderly. *Geriatric Rheumatology* Springer; 2011:287-291.

8 Bowman RJ, Dickerson M, Mwende J, Khaw PT. Outcomes of goniotomy for primary congenital glaucoma in East Africa. *Ophthalmology* 2011;118(2):236-240.

9 Wu LL, Huang P, Gao YX, Wang ZX, Li B. A 12-week, double-masked, parallel-group study of the safety and efficacy of travoprost 0.004% compared with pilocarpine 1% in Chinese patients with primary angle-closure and primary angle-closure glaucoma. *J Glaucoma* 2011;20(6):388-391.

10 Turski L, Cavalheiro EA, Czuczwar SJ, Turski WA, Kleinrok Z. The seizures induced by pilocarpine: behavioral, electroencephalographic and neuropathological studies in rodents. *Pol J Pharmacol* 1987;39(5):545-555.

11 Phillips CI, Clark CV, Levy AM. Posterior synechiae after glaucoma operations: aggravation by shallow anterior chamber and pilocarpine. *Br J Ophthalmol* 1987;71(6):428-432.

12 Kuchenbecker J, Motschmann M, Schmitz K, Behrens-Baumann W. Laser iridocystotomy for bilateral acute angle-closure glaucoma secondary to iris cysts. *Am J Ophthalmol* 2000;129(3):391-393.

13 Everitt DE, Avorn J. Systemic effects of medications used to treat glaucoma. *Ann Intern Med* 1990;112(2):120-125.

14 Kanjilal B, Keyser BM, Andres DK, Nealley E, Benton B, Melber AA, Andres JF, Letukas VA, Clark O, Ray R. Differentiated NSC-34 cells as an in vitro cell model for VX. *Toxicol Mech Methods* 2014;24(7):488-494.

15 Fan TJ, Hu XZ, Zhao J, Niu Y, Zhao WZ, Yu MM, Ge Y. Establishment of an untransfected human corneal stromal cell line and its biocompatibility

to acellular porcine corneal stroma. *Int J Ophthalmol* 2012;5(3):286-292.

16 Yu HZ, Li YH, Wang RX, Zhou X, Yu MM, Ge Y, Zhao J, Fan TJ. Cytotoxicity of lidocaine to human corneal endothelial cells in vitro. *Basic Clin Pharmacol* 2014;114(4):352-359.

17 Lee PY, Costumbrado J, Hsu CY, Kim YH. Agarose gel electrophoresis for the separation of DNA fragments. *J Vis Exp* 2012;(62):pii: 3923.

18 Sen E, Nalcacioglu P, Yazici A, Aksakal FN, Altinok A, Tuna T, Koklu G. Comparison of the effects of latanoprost and bimatoprost on central corneal thickness. *J Glaucoma* 2008;17(5):398-402.

19 Amano S, Nakai Y, Ko A, Inoue K, Wakakura M. A case of keratoconus progression associated with the use of topical latanoprost. *Jpn J Ophthalmol* 2008;52(4):334-336.

20 Zhou X, Li YH, Yu HZ, Wang RX, Fan TJ. Local anesthetic lidocaine induces apoptosis in human corneal stromal cells in vitro. *Int J Ophthalmol* 2013;6(6):766-771.

21 Wen Q, Fan T, Bai S, Sui Y. Cytotoxicity of proparacaine to human corneal endothelial cells in vitro. *J Toxicol Sci* 2015; 40(4):427-436.

22 Tian CL, Wen Q, Fan TJ. Cytotoxicity of atropine to human corneal epithelial cells by inducing cell cycle arrest and mitochondrion dependent apoptosis. *Exp Toxicol Pathol* 2015;67(10): 517-524.

23 Li YH, Wen Q, Fan TJ, Ge Y, Yu MM, Sun LX, Zhao Y. Dose dependent cytotoxicity of pranoprofen in cultured human corneal endothelial cells by inducing apoptosis. *Drug Chem Toxicol* 2015;38(1):16-21.

24 Miao Y, Sun Q, Wen Q, Qiu Y, Ge Y, Yu MM, Fan TJ. Cytotoxic effects of betaxolol on healthy corneal endothelial cells both in vitro and in vivo and in vivo. *Int J Ophthalmol* 2014;7(1):14-21.

25 Lobner D. Comparison of the LDH and MTT assays for quantifying cell death: validity for neuronal apoptosis? *J Neurosci Methods* 2000;96 (2): 147-152.

26 Ciniglia C, Pinto G, Sansone C, Pollio A. Acridine orange/ethidium bromide double staining test: a simple in-vitro assay to detect apoptosis induced by phenolic compounds in plant cells. *Allelopathy J* 2010;26(2): 301-308.

27 Vermes I, Haanen C, Steffens-Nakken H, Reutelingsperger C. A novel assay for apoptosis. Flow cytometric detection of phosphatidylserine early apoptotic cells using fluorescein labeled expression on Annexin V. *J Immunol Methods* 1995;184(1):39-51.

28 Oberhammer F, Wilson JW, Dive C, Morris ID, Hickman JA, Wakeling AE, Walker PR, Sikorska M. Apoptotic death in epithelial cells: cleavage of DNA to 300 and/or 50 kb fragments prior to or in the absence of internucleosomal fragmentation. *EMBO J* 1993;12(9):3679-3684.

29 Brustmann H. Apoptotic bodies as a morphological feature in serous ovarian carcinoma: correlation with nuclear grade, Ki-67 and mitotic indices. *Pathol Res Pract* 2002;198(2):85-90.

30 Jin Z, El-Deiry WS. Overview of cell death signaling pathways. *Cancer Biol Ther* 2005:4(2):139-163.

31 Spierings D, McStay G, Saleh M, Bender C, Chipuk J, Maurer U, Green DR. Connected to death: the (unexpurgated) mitochondrial pathway of apoptosis. *Science* 2005;310(5745):66-67.

32 Kumar S, Vaux DL. Apoptosis. A cinderella caspase takes center stage. *Science* 2002;297(5585):1290-1291.

33 Fan T, Han L, Cong RS, Liang J. Caspase family proteases and apoptosis. *Acta Biochim Biophys Sin (Shanghai)* 2005;37(11):719-727.

34 Brenner C, Kroemer G. Apoptosis. Mitochondria--the death signal integrators. *Science* 2000;289(5482):1150-1151.

35 Cai J, Yang J, Jones DP. Mitochondrial control of apoptosis: the role of cytochrome c. *Biochim Biophys Acta* 1998;1366(1-2):139-149.

36 Pop C, Timmer J, Sperandio S, Salvesen GS. The apoptosome activates caspase-9 by dimerization. *Mol Cell* 2006;22(2):269-275.

37 Wajant H. The Fas signaling pathway: more than a paradigm. *Science* 2002;296(5573):1635-1636.

38 Sun XM, MacFarlane M, Zhuang J, Wolf BB, Green DR, Cohen GM. Distinct caspase cascades are initiated in receptor-mediated and chemical-induced apoptosis. *J Biol Chem* 1999;274(8):5053-5060.

39 Zhang FT, Ding Y, Shah Z, Xing D, Gao Y, Liu DM, Ding MX. TNF/TNFR1 pathway and endoplasmic reticulum stress are involved in ofloxacin-induced apoptosis of juvenile canine chondrocytes. *Toxicol Appl Pharmacol* 2014;276(2):121-128.